0026-895X/06/7004-1204–1211$20.00
MOLECULAR PHARMACOLOGY
Vol. 70, No. 4
26203/3140558
Mol Pharmacol 70:1204–1211, 2006
Printed in U.S.A.

Binding Site of a Novel Kv1.5 Blocker: A "Foot in the Door" against Atrial Fibrillation

Niels Decher, Pradeep Kumar, Teresa Gonzalez, Bernard Pirard, and Michael C. Sanguinetti

Nora Eccles Harrison Cardiovascular Research and Training Institute and Department of Physiology, University of Utah, Salt Lake City, Utah (N.D., P.K., T.G., M.C.S.); Institut für Normale und Pathologische Physiologie, Universität Marburg, Marburg, Germany (N.D.); and Sanofi-Aventis Deutschland GmbH, Frankfurt am Main, Germany (B.P.)

Received May 1, 2006; accepted July 11, 2006

ABSTRACT

Kv1.5 channel blockers prolong atrial action potentials and may prevent atrial flutter or fibrillation without affecting ventricular repolarization. Here we characterize the mechanisms of action of 2′-{[2-(4-methoxy-phenyl)-acetylamino]-methyl}-biphenyl-2-carboxylic acid (2-pyridin-3-yl-ethyl)-amide (AVE0118) on Kv1.5 channels heterologously expressed in *Xenopus laevis* oocytes. Whole cell currents in oocytes were recorded using the two-microelectrode voltage clamp technique. AVE0118 blocked Kv1.5 current in oocytes with an IC_{50} of 5.6 μM. Block was enhanced by higher rates of stimulation, consistent with preferential binding of the drug to the open state of the channel. Ala-scanning mutagenesis of the pore domain of Kv1.5 identified the amino acids Thr479, Thr480, Val505, Ile508, Val512, and Val516 as important residues for block by AVE0118. A homology model of the pore region of Kv1.5 predicts that these six residues face toward the central cavity of the channel. In addition, mutation of two other S6 residues (Ile502 and Leu510) that are predicted to face away from the central cavity also diminished drug block. All these putative drug-binding residues are highly conserved in other Kv channels, explaining our finding that AVE0118 also blocked Kv1.3, Kv2.1, Kv3.1, and Kv4.3 channels with similar potency. Docking of AVE0118 into the inner cavity of a Kv1.5 pore homology model predicted an unusual binding mode. The drug aligned with the inner S6 α-helical domain in a manner predicted to block the putative activation gate. This "foot-in-the-door" binding mode is consistent with the observation that the drug slowed the rate of current deactivation, causing a crossover of tail current traces recorded before and after drug treatment.

Atrial fibrillation represents a major clinical problem that can result in serious morbidity in elderly persons (Chugh et al., 2001). Kv1.5 channels conduct the ultrarapid delayed rectifier current (I_{Kur}) that mediates repolarization of action potentials in the human atria (Fedida et al., 1993; Snyders et al., 1993). Reduction of this current prolongs atrial action potential duration and may prevent atrial flutter and fibrillation. Therefore, the pharmaceutical industry has developed novel Kv1.5 blockers to prevent and treat atrial arrhythmia (Peukert et al., 2003). I_{Kur} density is large in the atria but small or absent in ventricular myocytes (Nerbonne, 2000). Thus, specific Kv1.5 blockers do not substantially prolong ventricular repolarization or prolong the QT interval, a problematic side effect of many other common medications.

This work was supported by National Institutes of Health/National Heart, Lung, and Blood Institute grant HL55236.
Article, publication date, and citation information can be found at http://molpharm.aspetjournals.org.
doi:10.1124/mol.106.026203.

The molecular determinants of the binding site for drugs that block Kv1.5 channels have been extensively studied. Quinidine, bupivacaine, and benzocaine interact with residues located near the pore helix (Thr479) and in the S6 domain (Thr507, Leu510, and Val514) of Kv1.5 (Snyders et al., 1992; Snyders and Yeola, 1995; Yeola et al., 1996; Franqueza et al., 1997; Caballero et al., 2002). More recently discovered Kv1.5 blockers, such as the anthranilic acid derivative S0100176, have also been shown to bind to residues located in the channel pore. Mutational analyses indicate that Thr479 and Thr480 located at the base of the pore helix and Val505, Ile508, and Val512 located in S6 mediate S0100176-induced blockage of Kv1.5 channels (Decher et al., 2004). The positions of these residues correspond to amino acids that determine drug binding to other voltage-gated K (Kv) channels such as hERG (Mitcheson et al., 2000), KCNQ1 (Seebohm et al., 2003), and Kv1.3 (Hanner et al., 2001).

In this study, we analyzed the blocking characteristics of

ABBREVIATIONS: S0100176, *N*-benzyl-*N*-pyridin-3-ylmethyl-2-(toluene-4-sulfonylamino)-benzamide hydrochloride; Kv, voltage-gated K^+; AVE0118, 2′-{[2-(4-methoxy-phenyl)-acetylamino]-methyl}-biphenyl-2-carboxylic acid (2-pyridin-3-yl-ethyl)-amide; cRNA, complementary RNA; WT, wild-type.

AVE0118, a nonspecific Kv1.5 blocker and novel antiarrhythmic drug. The compound induces a rapid block of Kv1.5 channel current (IC_{50} = 1.1 μM) during a depolarizing pulse in Chinese hamster ovary cells, consistent with preferential block of open channels (Gogelein et al., 2004). AVE0118 blocks several ion channels in addition to Kv1.5 (Gogelein et al., 2004); however, the net effect of the drug is prolongation of atrial effective refractory period and reduction of electrical stimulation-induced atrial tachyarrhythmia in pigs (Wirth et al., 2003). AVE0118 also reduced the inducibility of atrial fibrillation in remodeled atria of the goat (Blaauw et al., 2004). Here we use Ala-scanning mutagenesis and voltage clamp analysis of mutant Kv1.5 channels expressed in *Xenopus laevis* oocytes to identify residues within the channel pore that interact with AVE0118. Our findings indicate that the putative binding site for this compound partially overlaps with S0100176 but includes other residues located in the S6 domain. The location of the binding site and docking of the drug to a homology model of the Kv1.5 pore region is consistent with our observation that AVE0118, but not S0100176, blocks Kv1.5 channels by a "foot-in-the-door" mechanism first described by Armstrong (1971) for block of squid axon delayed rectifier K^+ current by quaternary ammonium compounds.

Materials and Methods

Molecular Biology. Polymerase chain reaction-based site-directed mutagenesis was used to introduce mutations into the human Kv1.5 (*KCNA5*) cDNA. Kv1.5 was cloned from human heart and differs from the database entry NM_002234 by two residues, K418R and K565E. The newer database entry of the Kv1.5 sequence (NM_002234) has an N terminus with two additional residues. This results in a shift of the amino acid numbering of +2, compared with literature referring to the previous entry (M60451). Polymerase chain reaction products were fully sequenced (ABI 3100; Applied Biosystems, Foster City, CA). Complementary RNA (cRNA) for injection into oocytes was prepared with T7 Capscribe (Roche, Indianapolis, IN) after linearization with NheI. Estimates of cRNA quality and quantity were determined by gel electrophoresis and UV spectroscopy.

Isolation, Injection, and Voltage Clamp of Oocytes. Stage IV and V *X. laevis* oocytes were isolated and injected with cRNA encoding wild-type (WT) or mutant Kv1.5 channels. Oocytes were injected with 2.5 to 12.5 ng of Kv1.5 cRNA and cultured in Barth's solution supplemented with 50 μg/ml gentamicin and 1 mM pyruvate at 18°C for 1 to 3 days before use in voltage clamp experiments. Barth's solution contained 88 mM NaCl, 1 mM KCl, 0.4 mM $CaCl_2$, 0.33 mM $Ca(NO_3)_2$, 1 mM $MgSO_4$, 2.4 mM $NaHCO_3$, and 10 mM HEPES, pH 7.4. For voltage clamp experiments, oocytes were bathed in a modified ND96 solution containing 96 mM NaCl, 4 mM KCl, 1 mM $MgC1_2$, 1 mM $CaC1_2$, and 5 mM HEPES, pH 7.6.

Voltage Clamp Protocols. Currents were recorded at room temperature (23–25°C) with standard two-microelectrode voltage clamp techniques (Stühmer, 1992). The holding potential was −80 mV. The interpulse interval for all the protocols was 10 s or longer to allow channels to fully recover from inactivation between pulses. To obtain current-voltage relationships and activation curves, 1.5-s voltage steps were applied in 10-mV increments to potentials that varied from −60 to +70 mV, followed by repolarization to −40 mV. The ratio of current in the presence of drug divided by current before drug ($I_{drug}/I_{control}$) was determined to calculate the fraction of unblocked current as a function of time. The time constant of current block (τ_b) was determined by fitting $I_{drug}/I_{control}$ to a monoexponential function. The frequency dependence of peak current block was analyzed by stepping for 250 ms to 0 mV at a pulse frequency that ranged from 1 to 3 Hz. At a frequency of 4 Hz, a pulse duration of 200 ms was used. The voltage dependence of Kv1.5 channel activation (with or without AVE0118) was determined from tail current analyses at −40 mV. The resulting relationship between test voltage (V_t) and normalized tail current (I_n) was fit to a Boltzmann equation to obtain the half-point ($V_{1/2}$) and slope factor (k): $I_n = 1/\{1 + \exp[(V_{1/2} - V_t)/k]\}$. Other voltage pulse protocols are described under *Results* and figure legends.

Data Analysis. pCLAMP 8 (Molecular Devices, Sunnyvale, CA) and Origin 7 (OriginLab Corp, Northampton, MA) software were used for data acquisition and analysis on a Dell Optiplex GX150 personal computer. All the fitting procedures were based on the simplex algorithm. The concentration required for 50% block of current (IC_{50}) was determined from Hill plots using three to five con-

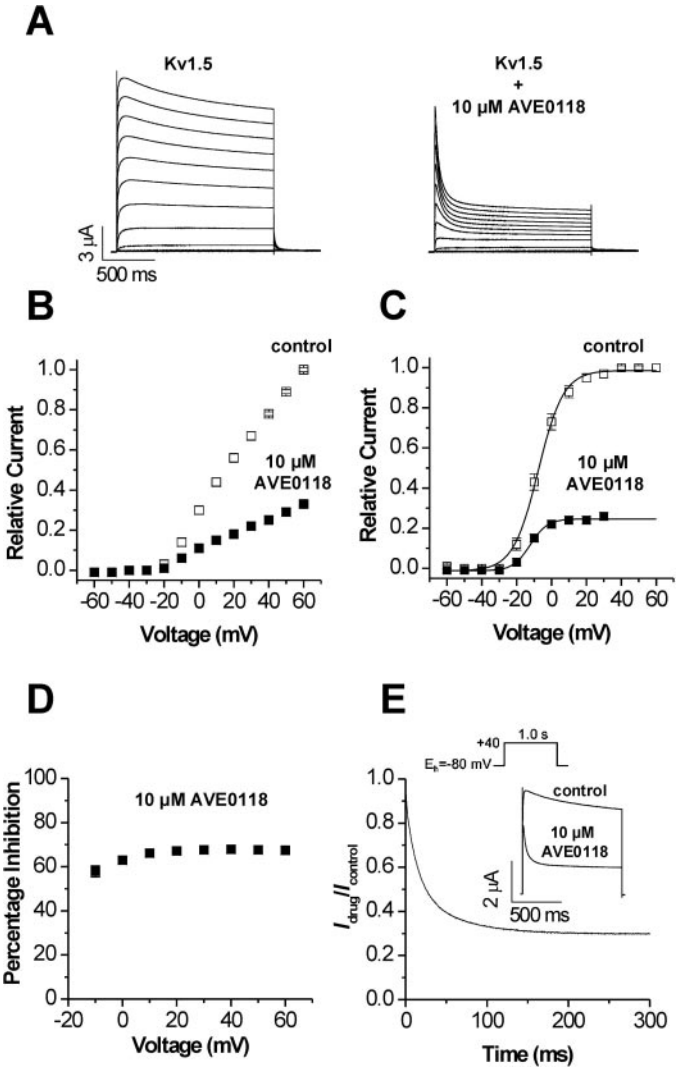

Fig. 1. Inhibition of Kv1.5 channel currents in *X. laevis* oocytes by 10 μM AVE0118. A, representative Kv1.5 currents recorded in a single oocyte before (left) and after (right) treatment of the same oocyte with AVE0118. B, current-voltage relationships for peak Kv1.5 current in the absence and presence of AVE0118. C, relative tail current amplitudes measured in absence and presence of drug. Tail currents were normalized to the peak value under control conditions for each oocyte. The smooth curves were obtained by fitting average data to a Boltzmann function. In control, the $V_{1/2}$ was −7.7 ± 0.6 mV, and the slope factor was 7.2 ± 0.5 mV; in the presence of drug, $V_{1/2}$ was −12.2 ± 0.6 mV, and the slope factor was 4.9 ± 0.5 mV (n = 11). D, percent inhibition of Kv1.5 current by 10 μM AVE0118 as a function of test voltage (n = 11). E, onset of current block. The time constant for block was 47.1 ± 0.5 ms.

centrations of drug for each mutant (3–10 oocytes/point). Results are reported as mean ± S.E.M. (n = number of oocytes). Statistical differences between WT and mutant channels were evaluated by a Student's unpaired t test. Significance was assumed for $P < 0.05$.

Homology Modeling of the Kv1.5 and hERG Pore and Docking of S0100176 and AVE0118. The pore-forming domains (S5–S6) of Kv1 channels share 54% sequence homology with the bacterial K^+ channel KcsA, whose three-dimensional structure has been solved by X-ray crystallography (Doyle et al., 1998). An open-state molecular model of the S5 to S6 region of Kv1.3 (provided by Dr. Ying-Duo Gao, Merck Research Laboratories, Rahway, NJ), generated using the crystal structure of the KcsA channel (Hanner et al., 2001) from the Protein Data Bank (code 1bl8), was used as a template for docking of drugs. The S5 and S6 domains and the pore helix of Kv1.3 and Kv1.5 share 100% sequence similarity.

The details of the ligand docking procedure have been described previously (Decher et al., 2004). We used GOLD (Jones et al., 1995) to dock drugs in the homology model of Kv1.5. For each docking, 25 poses were generated and ranked by the GOLDSCORE scoring function. Visual inspection of these poses guided selection of the pose with the highest GOLDSCORE fitness value and the lowest number of bumps with the protein for subsequent minimization. A two-step energy minimization protocol was applied: 1) 100 steps, steepest descent energy minimization, and 2) 5000 steps, Powell minimization. At each stage, the energy was evaluated by the MMF94S force field as implemented in SYBYL 7.0 (Tripos, St. Louis, MO). For these calculations, we used the MMF94S charges and a distance-dependent dielectric constant of 4r (where r is the distance). The minimized poses were visually inspected, and the amino acids within 4.5 Å of the docked compound were identified.

Drugs. AVE0118 and S0100176 were synthesized by the medicinal chemistry department of Sanofi-Aventis Deutschland GmbH. They were prepared as a 50 mM stock solution in dimethyl sulfoxide and stored at room temperature.

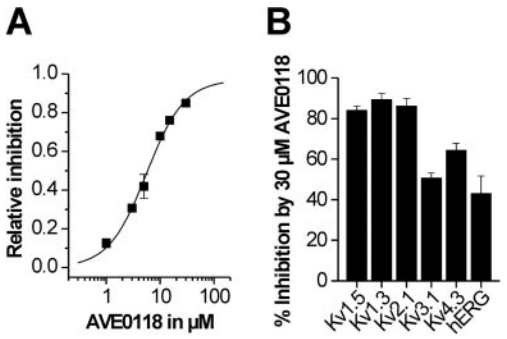

Fig. 2. AVE0118 is a nonspecific Kv channel blocker. A, concentration-effect relationship for Kv1.5 block by AVE0118. B, comparison of block of Kv1.5 with five other Kv channels by 30 μM AVE0118. Block of Kv1.5, Kv1.3, and Kv3.1 currents was determined during repetitive 1-s pulses to +40 mV from a holding potential of −80 mV, applied at a frequency of 0.083 Hz. Kv4.3 currents were elicited with the same pulse protocol, but current magnitude was calculated by integration over the initial 250 ms, the time required for ~90% inactivation. hERG currents were elicited with 2.5-s pulses to 0 mV, applied at a frequency of 0.2 Hz from a holding potential of −90 mV. hERG current magnitude was measured as peak tail currents measured at −70 mV.

Results

Voltage and Frequency-Dependent Block of Kv1.5 Channels by AVE0118. The effect of 10 μM AVE0118 on Kv1.5 was characterized by eliciting currents with step changes in voltage to potentials ranging from −60 to +60 mV, applied in 10-mV increments from a holding potential of −80 mV. In the absence of drug, Kv1.5 slowly inactivates during the test pulse (Fig. 1A). In the presence of drug, the current seemed to inactivate much faster and more thoroughly, but this effect more likely represents open channel block rather than an increased rate of inactivation. Current was blocked at all the test potentials (Fig. 1B), and there was only a small shift in the voltage dependence of activation for currents measured at the end of the 1.5-s pulse (Fig. 1C). The $V_{1/2}$ for activation was −7.7 ± 0.6 mV before and −12.2 ± 0.6 mV after 10 μM AVE0118 (n = 7). Current reduction was not voltage-dependent when measured at the end of the 1.5-s pulse (Fig. 1D). The lack of an increase in block at higher potentials suggests that this compound does not preferentially block Kv1.5 channels in the inactivated state.

To determine whether block of Kv1.5 by AVE0118 requires channel opening, we recorded currents in oocytes before and after a pulse-free period of incubation with the compound. Specifically, Kv1.5 currents were elicited at a test potential of +40 mV from a holding potential of −80 mV before and after exposure of an oocyte to 10 μM AVE0118 for 8 min without pulsing. The initial value of the $I_{drug}/I_{control}$ relationship (Fig. 1E) suggests a tonic block of 10% and that further block to a steady-state value of ~70% developed during the initial 300-ms duration of the pulse. Alternatively, the apparent

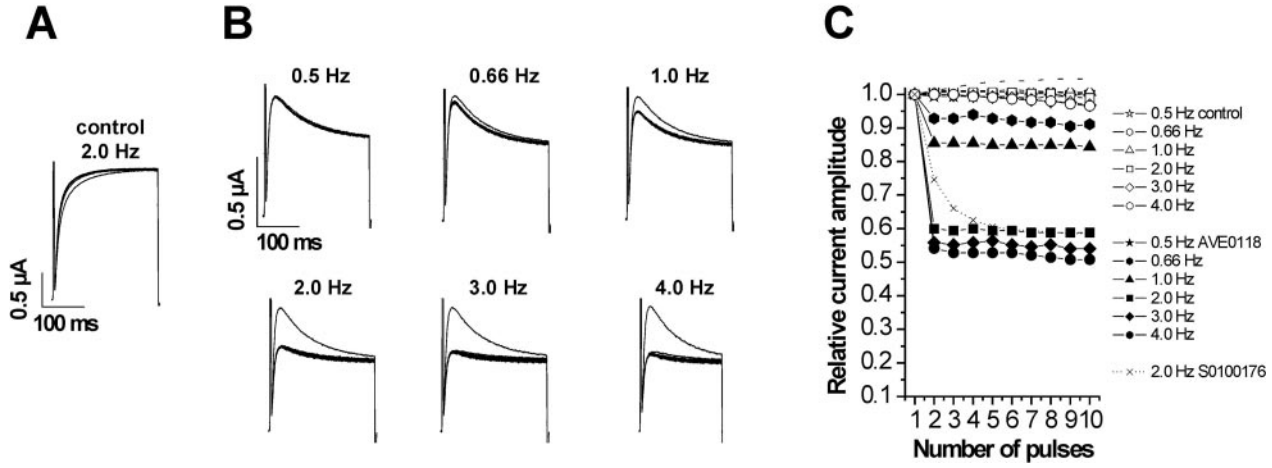

Fig. 3. Frequency-dependent block of Kv1.5 by AVE0118. A, Kv1.5 currents are not significantly altered during a train of pulses applied at 2 Hz. B, Kv1.5 currents elicited by 10 repetitive test pulses to 0 mV at a pulse frequency of 0.5 to 4 Hz in the presence of 10 μM AVE0118. C, plot of frequency-dependent changes in relative peak Kv1.5 currents before and after treatment of oocytes with 10 μM AVE0118.

tonic block may represent an extremely fast phase of open channel block.

The concentration of compound required to reduce Kv1.5 current by 50% (IC_{50}) at the end of a 1.5-s pulse to +40 mV was 5.6 ± 0.4 μM with a Hill coefficient of 1.23 (n = 3–10) (Fig. 2A). As reported previously (Gogelein et al., 2004), AVE0118 is not a specific Kv1.5 blocker. Kv1.3 and Kv2.1 channels had a sensitivity that was similar to Kv1.5 channels (85–90% block at 30 μM), whereas Kv3.1 and Kv4.3 channels were less sensitive (Fig. 2B). In addition, 30 μM AVE0118 blocked hERG channels by ~40%. Thus, AVE0118 is nonspecific and blocks several Kv channels.

Use Dependence of Kv1.5 Block by AVE0118. A common property of an open channel blocker is use dependence that reflects the dynamics of the on and off rates for drug binding. Consistent with open channel block, the inhibition of peak Kv1.5 was dependent on the pulse frequency. Currents were recorded in the absence or presence of 10 μM AVE0118 during voltage steps applied at a frequency of 0.5, 0.66, 1, 2, 3, and 4 Hz to a potential of 0 mV. At this voltage and in the absence of drug, Kv1.5 did not exhibit measurable inactivation during 250-ms pulses applied at 2 Hz (Fig. 3A). In the presence of drug, current decreased as a function of pacing rate (Fig. 3B). Normalized peak current amplitudes at different frequencies were plotted as a function of the pulse number (Fig. 3C). In the absence of AVE0118, Kv1.5 currents decreased by 0.5 ± 0.2, 1.9 ± 0.4, 4.1 ± 2.8, 7.6 ± 3.1, 10.1 ± 4.8, and 11.2 ± 6.4% (n = 5) when recorded with trains of pulses applied at 0.5, 0.66, 1, 2, 3, and 4 Hz, respectively. In the presence of 10 μM AVE0118, peak current was reduced by 9.8 ± 2.7% (n = 5) when pulses were applied at the very slow frequency of 0.0333 Hz. The normalized currents were suppressed by an additional 8.1 ± 1.9, 15.3 ± 2.6, 39.0 ± 3.1, 45.2 ± 2.9, and 48.7 ± 3.4% (n = 5) at 0.66, 1, 2, 3, and 4 Hz,

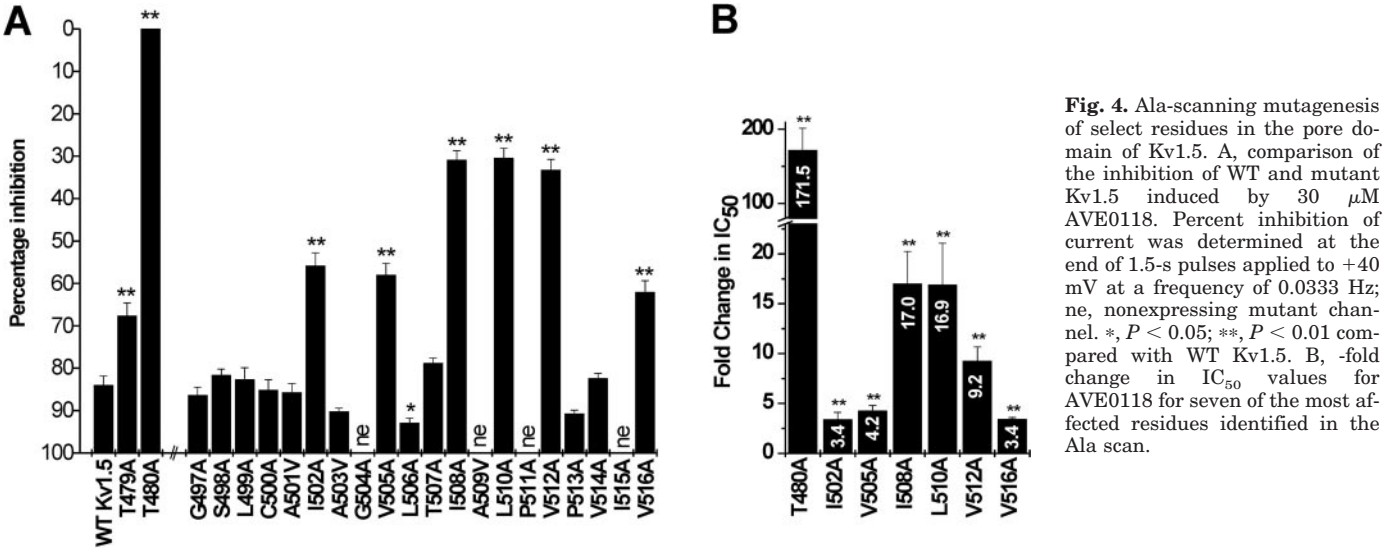

Fig. 4. Ala-scanning mutagenesis of select residues in the pore domain of Kv1.5. A, comparison of the inhibition of WT and mutant Kv1.5 induced by 30 μM AVE0118. Percent inhibition of current was determined at the end of 1.5-s pulses applied to +40 mV at a frequency of 0.0333 Hz; ne, nonexpressing mutant channel. *, $P < 0.05$; **, $P < 0.01$ compared with WT Kv1.5. B, -fold change in IC_{50} values for AVE0118 for seven of the most affected residues identified in the Ala scan.

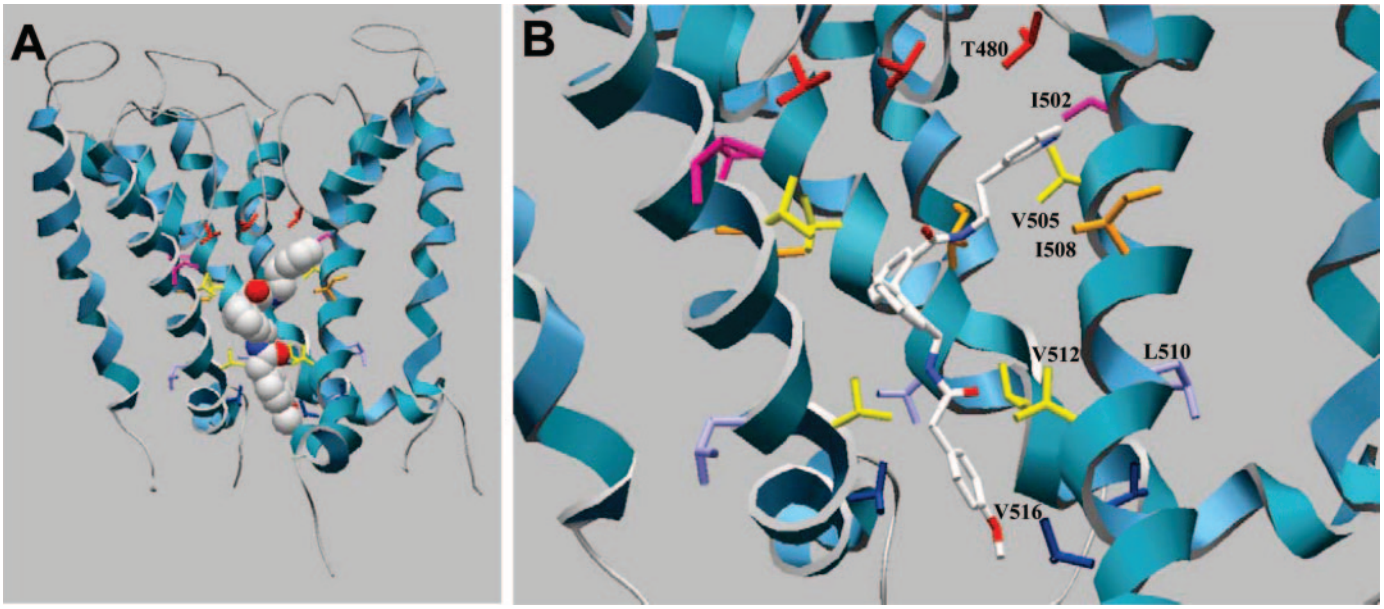

Fig. 5. Simulated docking of AVE0118 to a pore homology model of Kv1.5. A, view of three subunits of the pore region (S5–S6) of Kv1.5 with AVE0118 portrayed as a space-fill model. B, close-up view of the central cavity of Kv1.5 with AVE0118 shown as a stick model. The key residues in the S6 domain (inner helix of each subunit) identified by the Ala scan are highlighted and labeled on one subunit.

respectively. Block of Kv1.5 by AVE0118 reached its steady state after a single pulse at all the frequencies (Fig. 3C). By contrast, we previously found that block of Kv1.5 by S0100176 required approximately 10 pulses to reach a steady state when the cell was pulsed at 2 to 4 Hz (Decher et al., 2004). Frequency-dependent block of Kv1.5 would be an advantageous property for an antifibrillatory drug because channels would be least affected during normal heart rates and most affected during the tachycardia.

Ala-Scanning Mutagenesis of Kv1.5 Pore Region. Residues located in the S6 domain or between the pore helix and the selectivity filter were chosen for the Ala scan based on their proximity to the central cavity, as described previously (Decher et al., 2004). Nineteen residues were mutated to Ala, and the two Ala residues in this region (Ala501, Ala509) were mutated to Val. AVE0118 was applied at a single concentration of 30 μM, and inhibition of Kv1.5 currents was analyzed at the end of 1.5-s test pulses to +40 mV. At this concentration, wild-type Kv1.5 channels were inhibited by 85% (Fig. 4). Because L510A Kv1.5 channels exhibited pronounced inactivation, we analyzed the inhibition of peak current amplitudes at +40 mV for this mutant. The P513A mutation caused a large rightward shift in the voltage of activation ($V_{1/2}$ near +70 mV); therefore, block was assessed at a test potential of +60 mV. The potency of AVE0118 block was significantly reduced ($P < 0.01$) by eight mutations (Fig. 4A). Two of these mutations were in residues located at the base of the pore helix near the selectivity filter (Thr479, Thr480). Six mutations were in residues located in the S6 segment (Ile502, Val505, Ile508, L510A, Val512, and Val516). The IC_{50} for AVE0118 was determined for these mutant channels except Thr479 (Fig. 4B). The IC_{50} was increased the most for T480A (172-fold), I508A (17-fold), and L510A (17-fold).

Model of AVE0118 Docking to the Kv1.5 Channel Pore. The ligand docking solution that passed several filtering steps (described under *Materials and Methods*) is presented in Fig. 5, A and B. The docking of the compound is illustrated from a side view facilitated by removal of one of the four subunits. The side chains of residues Thr480, Ile502, Val505, Ile508, Leu510, Val512, and Val516 from at least one

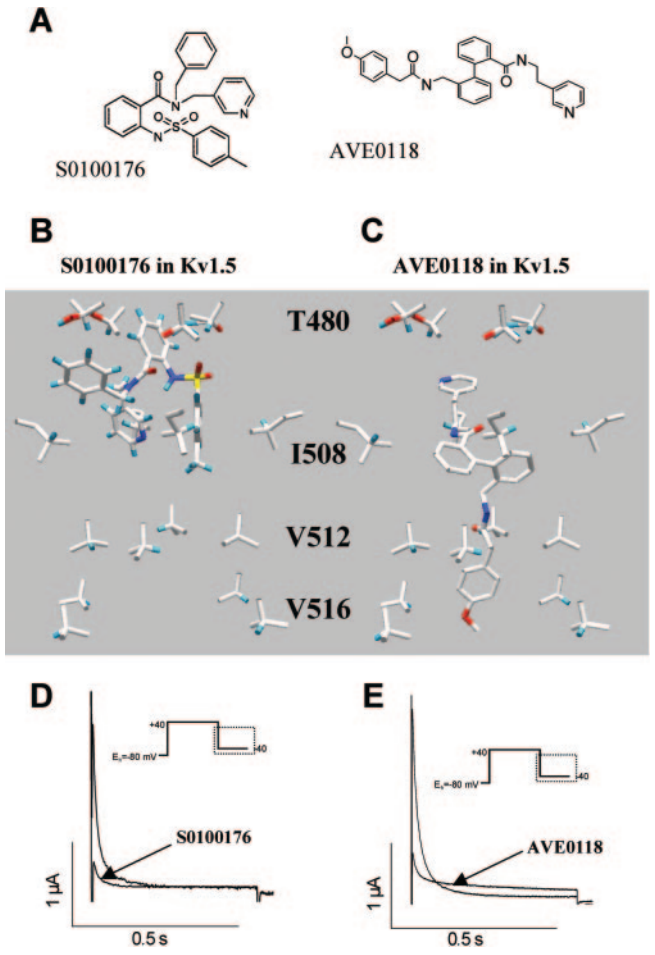

Fig. 6. Comparison of the docking modes of AVE0118 and S0100176 in the central cavity of the Kv1.5 homology model. A, chemical structures of AVE0118 and S0100176. B, energy-minimized S0100176 molecules surrounded by the side groups of specific residues proposed to comprise the drug binding site located in the central cavity. C, docking proposed for AVE0118. D and E, Kv1.5 tail currents recorded at −40 mV in oocytes before and after treatment with 3 μM S0100176 (D) or 10 μM AVE0118 (E). Note that tail currents exhibit crossover for AVE0118 but not for S0100176.

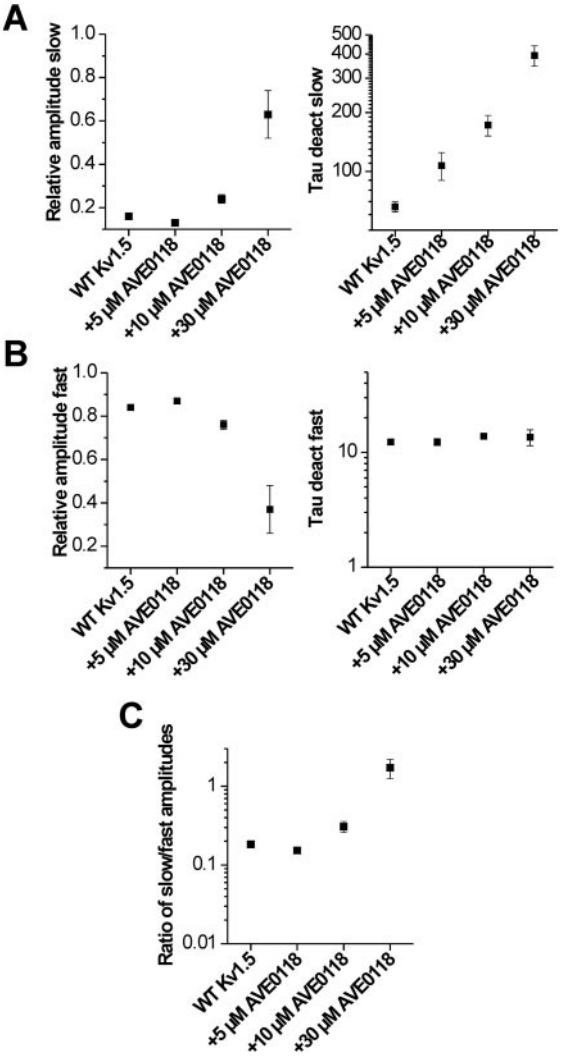

Fig. 7. Changes in Kv1.5 deactivation kinetics caused by AVE0118 are concentration-dependent. A, relative amplitudes and time constants for slow component of tail current deactivation at −40 mV. B, relative amplitudes and time constants for fast component of tail current deactivation at −40 mV. C, ratio of slow/fast tail current amplitudes.

subunit of the tetramer were predicted to be located within 4.5 Å of AVE0118. Seven of the nine mutations that reduced the sensitivity of Kv1.5 to block by AVE0118 were in residues that face toward the central cavity of the channel (Fig. 5). Only the side chains of Ile502 and Leu510 are positioned away from the central cavity.

The simulated positioning of AVE0118 within the pore of the Kv1.5 homology model differs significantly from the position previously determined for another Kv1.5 blocker, S0100176 (Decher et al., 2004). The chemical structures of the two compounds are shown in Fig. 6A, and their configuration relative to the important binding site residues is compared in Fig. 6, B and C. Unlike the more compactly shaped S0100176, AVE0118 is predicted to have a more elongated shape and have contacts with residues located near the C-terminal end of the S6 domain. These contrasting modes of binding for the two compounds are associated with differential effects on deactivation of Kv1.5 current. S0100176 did not change kinetics of Kv1.5 deactivation (Fig. 6D). By contrast, AVE0118 slowed deactivation, causing a crossover of the tail currents measured before and after treatment of oocytes with the compound (Fig. 6E).

Deactivation of WT Kv1.5 was biexponential at −40 mV with time constants 12.3 ± 0.5 and 65.8 ± 3.9 ms (n = 20). The relative amplitude of the fast component was 0.84 ± 0.01 before drug. As concentration of AVE0118 was increased from 5 to 10 to 30 μM, the slow component of deactivation became more prominent and its time constant slower (Fig. 7A). These changes were accompanied by a decrease in the relative amplitude of the fast component, but there was no change in time constant (Fig. 7B). Presumably, the component of current that deactivates fast represents the fraction of channels not affected by AVE0118. Finally, the ratio of the slow to fast components of deactivation was increased by the drug (Fig. 7C). Thus, consistent with a foot-in-the-door mechanism, the slowing of deactivation and increase in the fraction of current that deactivates slowly was dependent on the concentration of AVE0118.

Changes in Drug Affinity Are Independent of Kv1.5 Inactivation. The L510A mutation reduced sensitivity to AVE0118 and caused a pronounced enhancement of C-type inactivation, reducing current by 80% during a 1.5-s pulse to +70 mV. By contrast, mutation of Leu510 to Met (L510M) did not enhance C-type inactivation, and the channel retained its sensitivity to AVE0118 (Fig. 8A). The differential effects of L510A and L510M on drug affinity is probably not related to C-type inactivation. As shown in Fig. 8B, there was no apparent relationship (r = −0.08) between percentage inactivation determined at a test potential of +40 mV and percentage of current inhibition for the mutant channels studied. The hydrophobic volume of Met and Leu are similar and much larger than Ala. Thus, the hydrophobic surface area of the side chain of residue 510 is important for sensitivity of the channel to AVE0118.

Discussion

Like many other Kv1 channel blockers, AVE0118 preferentially blocks Kv1.5 channels in the open state. Our Ala-scanning mutagenesis results identified several residues located in the S6 domain (Val505, Ile508, Val512, and Val516) and Thr480 located near the base of the pore helix as critical components of the binding site for AVE0118. These six residues face toward the central cavity of the channel. Surprisingly, mutation to Ala of Leu510 (and to a lesser extent Ile502) in the S6 domain, a residue predicted to face toward S5 and away from the central cavity, also substantially reduced channel block by AVE0118. We previously found that mutation of Leu510 had no impact on S0100176 block (Decher et al., 2004). It is unclear why mutation of Leu510 specifically causes a change in AVE0118 sensitivity, but perhaps substitution of the large hydrophobic Leu residue with a much smaller Ala alters the orientation of the side chains of the nearby Ile508 and/or Val512 to impede interactions with this drug but not S0100176.

All the residues in Kv1.5 identified as important for drug block are highly conserved in other Kv channels. Thus, our findings that AVE0118 also blocked Kv1.3, Kv2.1, and Kv3.1 channels are not surprising. In addition, we confirmed (in oocytes) the findings of Gogelein et al. (2004) that AVE0118 also blocks Kv4.3 and hERG channels. Despite its nonselective nature, AVE0118 effectively prevents atrial fibrillation (Blaauw et al., 2004; Wettwer et al., 2004). Perhaps nonselective channel block by AVE0118 leads to an overall decrease in cardiac excitability, similar to the effects of the antiarrhythmic agent amiodarone on the ventricle. Like ami-

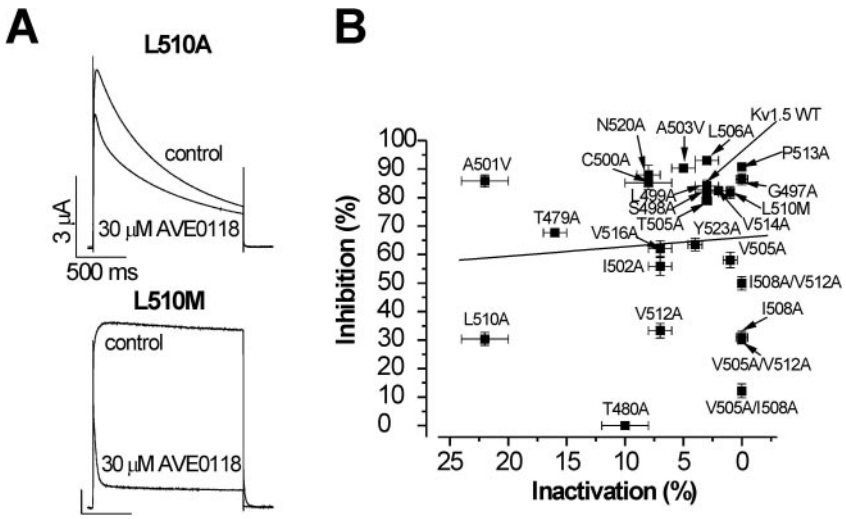

Fig. 8. Lack of correlation between block by AVE0118 and Kv1.5 channel inactivation. A, L510A and L510M Kv1.5 channel currents have different inactivation properties and sensitivity to block by 30 μM AVE0118. B, block of Kv1.5 mutant channel currents, expressed as percentage inhibition by 30 μM AVE0118 plotted versus the percentage of current inactivation at +40 mV for a 1.5-s pulse. Linear regression analysis indicated no correlation between the two variables (r = −0.08).

odarone, AVE0118 also blocks hERG channels (Gogelein et al., 2004); however, unlike amiodarone, it does not prolong QT interval (Blaauw et al., 2004). A possible explanation for this difference is that AVE0118 is a sufficiently effective L-type Ca^{2+} channel blocker compared with its generalized K^+ channel block (Gogelein et al., 2004), resulting in no net change in the rate of ventricular myocyte repolarization. The onset of Kv1.5 channel block by AVE0118 is very fast and highly rate-dependent. This profile of block may be advantageous for preventing initiation of atrial fibrillation.

Docking of AVE0118 to the Kv1.5 pore homology model revealed that the compound orients within the pore in a configuration that extends toward the cytoplasmic side of the channel beyond Val512 of the S6 domain. This extended configuration might impede closure of the channel by preventing the crisscrossing of the four S6 domains believed to represent the closed state of K^+ channels (Doyle et al., 1998). This mode of binding is consistent with our observation that AVE0118 slowed deactivation of Kv1.5 current, resulting in a crossover of tail current traces recorded in the absence and presence of the drug. This effect was first noted for quaternary ammonium compounds by Armstrong (1971), who suggested that a compound bound to the inner pore prevented normal closure of the activation gate (foot in the door) and that channels could only close after the drug dissociated from its binding site. The more compact shape of S0100176 when docked to the inner pore would not be expected to cause a foot-in-the-door effect (Fig. 9, A and B), consistent with our finding that this drug did not slow the rate of current deactivation.

Kvβ subunits can modulate the pharmacology of Kv1 channels in addition to their well characterized ability to alter channel gating and expression. For example, Kvβ1.3 subunits reduce the block of Kv1.5 by bupivacaine, quinidine, and S0100176 (Gonzalez et al., 2002; Decher et al., 2005). Our previous findings suggested that S0100176 and the Kvβ1.3 subunit compete for an overlapping but not identical binding site located in the inner cavity of Kv1.5 (Decher et al., 2005). Our present findings provide further evidence that Kv1 pore blockers contact the same subset of residues in the S6 domain. Interestingly, the amino acids that influence block by AVE0118 are located throughout the S6 segment and include residues Leu510 and Val516, similar to the binding site of Kvβ1.3, which also shows a foot-in-the-door slowing of deactivation. As implied by the dockings shown in Fig. 5 and Fig. 6, each drug may only interact with one of the S6 residues at each position in the tetrameric channel.

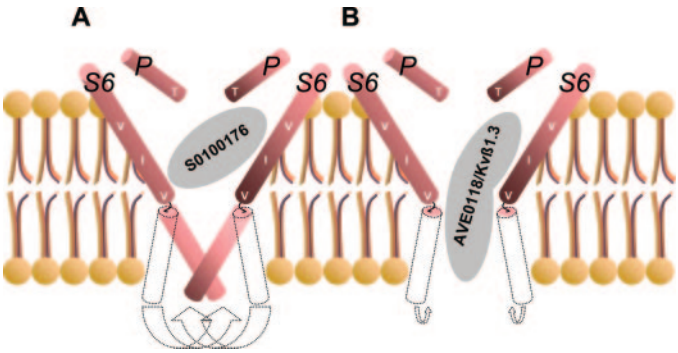

Fig. 9. Diagram illustrating proposed interactions of a drug or Kvβ subunit with an open or closed Kv1.5 channel. The approximate location of the key Val (V) and Ile (I) residues in the inner helix (S6) and the Thr (T) residue near the pore helix (P) are indicated. S0100176 bound to the channel is proposed to be trapped within the central cavity in the closed state (A). When AVE0118 or a Kvβ subunit is bound to the pore, the channel cannot close normally (B), a foot-in-the-door type of block.

In summary, we have defined the residues in the central cavity of Kv1.5 that make contact with AVE0118 and mediate its open state-dependent channel block. The inferred binding site significantly overlaps with the site we previously mapped for S0100176 and the N terminus of Kvβ1.3 subunits. It remains to be determined whether differences in rate of block onset or mode of trapping observed for different Kv1.5 blockers translate to advantages or disadvantages in the treatment and prevention of atrial fibrillation.

Acknowledgments

We thank Krista Kinard, Meng San Pun, Chandra Talluri, and Kam Ng Hoe for technical assistance and Jürgen Daut for continuous support of N.D.

References

Armstrong CM (1971) Interaction of tetraethylammonium ion derivatives with the potassium channels of giant axons. *J Gen Physiol* **58:**413–437.

Blaauw Y, Gogelein H, Tieleman RG, van Hunnik A, Schotten U, and Allessie MA (2004) "Early" class III drugs for the treatment of atrial fibrillation: efficacy and atrial selectivity of AVE0118 in remodeled atria of the goat. *Circulation* **110:**1717–1724.

Caballero R, Moreno I, Gonzalez T, Valenzuela C, Tamargo J, and Delpon E (2002) Putative binding sites for benzocaine on a human cardiac cloned channel (Kv1.5). *Cardiovasc Res* **56:**104–117.

Chugh SS, Blackshear JL, Shen WK, Hammill SC, and Gersh BJ (2001) Epidemiology and natural history of atrial fibrillation: clinical implications. *J Am Coll Cardiol* **37:**371–378.

Decher N, Kumar P, Gonzalez T, Renigunta V, and Sanguinetti MC (2005) Structural basis for competition between drug binding and Kvbeta 1.3 accessory subunit-induced N-type inactivation of Kv1.5 channels. *Mol Pharmacol* **68:**995–1005.

Decher N, Pirard B, Bundis F, Peukert S, Baringhaus KH, Busch AE, Steinmeyer K, and Sanguinetti MC (2004) Molecular basis for Kv1.5 channel block: conservation of drug binding sites among voltage-gated K^+ channels. *J Biol Chem* **279:**394–400.

Doyle DA, Morais Cabral J, Pfuetzner RA, Kuo A, Gulbis JM, Cohen SL, Chait BT, and MacKinnon R (1998) The structure of the potassium channel: molecular basis of K^+ conduction and selectivity. *Science (Wash DC)* **280:**69–77.

Fedida D, Wible B, Wang Z, Fermini B, Faust F, Nattel S, and Brown A (1993) Identity of a novel delayed rectifier current from human heart with a cloned K^+ channel current. *Circ Res* **73:**210–216.

Franqueza L, Longobardo M, Vicente J, Delpon E, Tamkun MM, Tamargo J, Snyders DJ, and Valenzuela C (1997) Molecular determinants of stereoselective bupivacaine block of hKv1.5 channels. *Circ Res* **81:**1053–1064.

Gogelein H, Brendel J, Steinmeyer K, Strubing C, Picard N, Rampe D, Kopp K, Busch AE, and Bleich M (2004) Effects of the atrial antiarrhythmic drug AVE0118 on cardiac ion channels. *Naunyn-Schmiedeberg's Arch Pharmacol* **370:**183–192.

Gonzalez T, Navarro-Polanco R, Arias C, Caballero R, Moreno I, Delpon E, Tamargo J, Tamkun MM, and Valenzuela C (2002) Assembly with the Kvbeta1.3 subunit modulates drug block of hKv1.5 channels. *Mol Pharmacol* **62:**1456–1463.

Hanner M, Green B, Gao YD, Schmalhofer WA, Matyskiela M, Durand DJ, Felix JP, Linde AR, Bordallo C, Kaczorowski GJ, et al. (2001) Binding of correolide to the K(v)1.3 potassium channel: characterization of the binding domain by site-directed mutagenesis. *Biochemistry* **40:**11687–11697.

Jones G, Willett P, and Glen RC (1995) Molecular recognition of receptor sites using a genetic algorithm with a description of desolvation. *J Mol Biol* **245:**43–53.

Mitcheson JS, Chen J, Lin M, Culberson C, and Sanguinetti MC (2000) A structural basis for drug-induced long QT syndrome. *Proc Natl Acad Sci USA* **97:**12329–12333.

Nerbonne JM (2000) Molecular basis of functional voltage-gated K^+ channel diversity in the mammalian myocardium. *J Physiol (Lond)* **525:**285–298.

Peukert S, Brendel J, Pirard B, Bruggemann A, Below P, Kleemann HW, Hemmerle H, and Schmidt W (2003) Identification, synthesis, and activity of novel blockers of the voltage-gated potassium channel Kv1.5. *J Med Chem* **46:**486–498.

Seebohm G, Chen J, Strutz N, Culberson C, Lerche C, and Sanguinetti MC (2003) Molecular determinants of KCNQ1 channel block by a benzodiazepine. *Mol Pharmacol* **64:**70–77.

Snyders D, Tamkun M, and Bennett P (1993) A rapidly activating and slowly inactivating potassium channel cloned from human heart. Functional analysis after stable mammalian cell culture expression. *J Gen Physiol* **101:**513–543.

Snyders DJ, Knoth KM, Roberds SL, and Tankun MM (1992) Time-, voltage-, and state- dependent block by quinidine of a cloned human cardiac potassium channel. *Mol Pharmacol* **41:**322–330.

Snyders DJ and Yeola SW (1995) Determinants of antiarrhythmic drug action. Electrostatic and hydrophobic components of block of the human cardiac hKv1.5 channel. *Circ Res* **77:**575–583.

Stühmer W (1992) Electrophysiological recording from *Xenopus* oocytes. *Methods Enzymol* **207:**319–339.

Wettwer E, Hala O, Christ T, Heubach JF, Dobrev D, Knaut M, Varro A, and Ravens U (2004) Role of IKur in controlling action potential shape and contractility in the human atrium: influence of chronic atrial fibrillation. *Circulation* **110:**2299–2306.

Wirth KJ, Paehler T, Rosenstein B, Knobloch K, Maier T, Frenzel J, Brendel J, Busch AE, and Bleich M (2003) Atrial effects of the novel K^+-channel-blocker AVE0118 in anesthetized pigs. *Cardiovasc Res* **60:**298–306.

Yeola SW, Rich TC, Uebele VN, Tamkun MM, and Snyders DJ (1996) Molecular analysis of a binding site for quinidine in a human cardiac delayed rectifier K^+ channel. *Circ Res* **78:**1105–1114.

Address correspondence to: Michael C. Sanguinetti, Nora Eccles Harrison Cardiovascular Research and Training Institute, University of Utah, 95 South 2000 East, Salt Lake City, UT 84112. E-mail: sanguinetti@cvrti.utah.edu